HIGH-INTENSITY LIGHT-ION BEAM RESEARCH AT NRL[+]

G. Cooperstein, R. J. Barker*, D. G. Colombant, A. Drobot**, Shyke A. Goldstein*, R. A. Meger*, D. Mosher, P. F. Ottinger*, F. L. Sandel*, S. J. Stephanakis and F. C. Young

Naval Research Laboratory, Washington, DC 20375

ABSTRACT

High-brightness proton beams (.4 MA, 1 MV) have recently been extracted from 20 cm^2 axial pinch-reflex diodes (PRDs) mounted on the NRL Gamble II generator. A source power brightness of > 10 TW/cm^2rad^2 was achieved in these experiments. A new barrel-shaped equitorial PRD that can be coupled to PBFA-II has also been operated on Gamble II and has demonstrated 50% proton efficiency with predominately azimuthally-symmetric charged-particle flow. In other experiments the stopping power of deuterons in hot plasmas was measured using a PRD on Gamble II. Results show about 40% enhancement in stopping power over that in cold targets when the beam was focused to about .25 MA/cm^2. Research is also being performed on transporting ion beams in large-diameter channels ($\gtrsim$ 2.5 cm) and on a post-transport, plasma-filled, magnetic-focusing section to bring the beam to pellet dimensions.

I. INTRODUCTION

Recent NRL experiments and theory have investigated key aspects of two ignition-system configurations for light-ion-drivers on PBFA-II.[1,2] The first configuration ties all 36 modules to a single barrel-shaped radial ion diode with 1 m dimensions surrounding the pellet located on the diode axis of symmetry. The barrel diameter must be small enough to permit focusing to pellet dimensions but large enough to permit time-of-flight bunching of the beam from the power-pulse duration to the pellet-driving time. The second configuration uses groups of modules to drive small-area disc-like axial ion diodes each of which focuses a beam into a z-discharge transport channel[3] about 2 m long and a few cm in diameter. Each channel is terminated in a short, higher-current discharge which magnetically focuses the beam onto the pellet.[2,4] Beam transport allows the diode focusing length to be much less than the bunching length and the post-transport magnetic-focusing allows larger-diameter beams to be transported and then focused. Such a system is schematically illustrated in Fig. 1

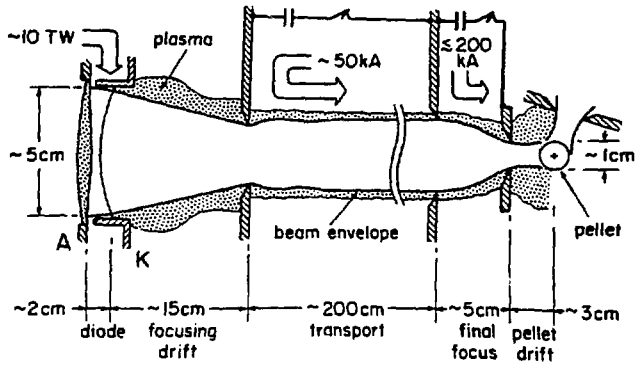

Fig. 1. Schematic of modular Light-Ion ICF system.

Ongoing research is evaluating pinch-reflex diodes (PRDs) for both ignition system configurations. Barrel-shaped equitorial PRD experiments on the NRL Gamble II device operating at 1.2 MV and .8 MA have demonstrated 50% proton efficiency with predominately azimuthally-symmetric charged-particle flow, average beam-divergence half-angles in the $1\text{-}2^{0}$ range between filaments, and good agreement with theoretical scaling laws.[5] This low divergence leads to a high brightness beam as defined in Sec. II. A high-power diode of similar design is now being tested on PBFA-II.[6] High-brightness proton beams (.4 MA, 1 MV) have recently been extracted from 20 cm^2 axial PRDs mounted on Gamble II. A source power brightness of 10 TW/cm^2rad^2 was achieved by minimizing the vacuum gap between the anode and cathode-transmission foils, thereby reducing the disruptive effects of filamentation in the vacuum gap.[7] Similar diodes have produced nearly 2 TW, 100 kJ proton and deuteron beams with 70% ion production efficiency on the Physics International PITHON generator.[8]

Other experiments on Gamble II have employed 20 cm^2 axial PRDs to measure the energy loss of deuteron beams in subrange Mylar and aluminum targets located at the beam focus. These targets are sandwiched between thin CD_2 layers so that ion-energy loss could be determined from time-of-flight analyses of the two neutron pulses. Results show about 40% enhancement in stopping power[9] over that in cold targets when the beam is focused to about .25 MA/cm^2. Results of these and other lower-current-density measurements are in excellent agreement with calculated stopping due to free and bound electrons at ionization levels expected from ion-target heating.[10] Factor-of-two enhancements over cold stopping for light- and heavy-ion beams are predicted at target temperatures expected for break-even pellets.

New stability constraints have recently been combined with channel-MHD and energy-loss constraints to define an operational window for transport of various light-ion species. Calculations of two-stream- and filamentation-instability growth rates show that multi-terawatt beams can be transported a few meters in channels a few centimeters in diameter.[2,11] Less than 10 channels would be sufficient to transport PBFA-II level beams and ignite a pellet provided that final magnetic focusing can be utilized to focus each transported beam. A proof-of-principle experiment for final focusing has been carried out on Gamble II using a 100 kA discharge channel 4 cm in diameter and 8 cm long mounted in front of the diode.[12] Experiments in which a transported beam will be focused are planned.

Section II will review recent high brightness diode experiments on Gamble II. The new barrel-shaped equitorial PRD concept and preliminary Gamble II results will be reviewed in Section III. Section IV will discuss the energy loss experiments of deuteron beams in subrange Mylar and aluminum targets. Finally transport considerations in large diameter channels and final focusing concepts and experiments will be discussed in Section V.

II. ION BEAM BRIGHTNESS STUDIES

Beam power brightness at the diode imposes the ultimate limit on the ability to focus ion beams onto targets. The PRD which has been previously described[13,14] and which is illustrated in Fig. 2 has been studied

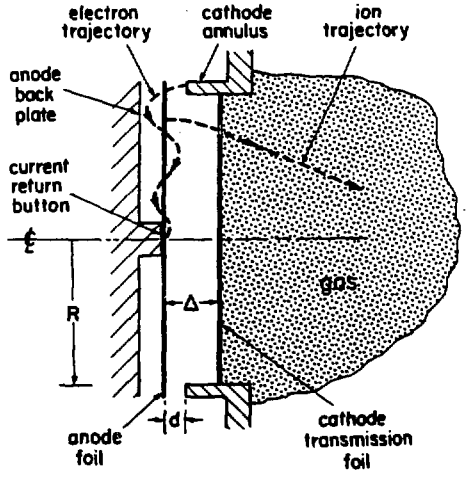

Fig. 2. Pinch-reflex-diode.

with respect to its performance as a source of high current density, low divergence ion beams. Both experimental and theoretical efforts are underway. Electron-filamentation instabilities which may occur in the electrode plasmas and vacuum gap are currently under investigation. Small-scale perturbations in diode electromagnetic fields associated with such instabilities can degrade brightness. In addition to their effects on beam brightness, varying electromagnetic fields and electrode-plasma motion also introduce time-dependent aberrations in the focusing properties of the diode. Changes in diode geometry and electrode materials are being investigated experimentally in order to determine their effects on the instabilities.

Provided that ion efficiency is not reduced and beam-divergence is not degraded, diode-beam brightness can be increased by reducing the diode radius. In recent 1 TW diode experiments on Gamble II, .6 TW proton beams were extracted from 20 cm^2-area anode foils. The ion beam brightness was measured crudely by a shadowbox technique[7] that uses multiple pinhole images of the ion beam. The recording plates used were either brass or cellophane. The brass is heated up by the impinging ion beam causing zinc to collect on the surface. Small features of ion beamlets can be clearly recorded provided their current density is high ($J_i \sim 10^3 A/cm^2$). The cellophane is more sensitive and records current densities down to 10 A/cm^2. Using these plates with the multiple hole shadowbox mounted far enough from the diode one can reconstruct the ion source pattern and its divergence. The ion source exhibited 10 to 20 beamlets for this small radius diode. Each beamlet had a size of about 1 cm in diameter. The beam divergence changed drastically when the gap, Δ, between the anode and the cathode inner foil was changed. The half angle of the diverging beam cone, $\delta\theta$, was measured to be $\sim .1$ rad at a gap of 1.5 cm and $\sim .05$ rad at a gap of .5 cm. The divergence was observed as a conic structure with no preference to radial or azimuthal direction.

A simple calculation to explain beam divergence versus gap width was performed assuming that the total ion beam current (450 kA) was distributed equally among 15 sources each having a diameter of 1 cm. Self-pinching of these ion beamlets by self-magnetic fields would result in $\delta\theta = .08\Delta/\sqrt{V}$ for protons at a voltage V measured in MV. The experimental results at V = 1.2 MV show that $\delta\theta$ agrees well with the predicted value at the larger gap of Δ=1.5 cm. At the smaller gap the plasma motion from the

cathode (2×10^6 cm/s) and anode (5×10^6 cm/s) reduce Δ from its initial value of .5 cm to a lower value of about .2 cm at peak power. The calculated divergence is then .015 rad compared with the observed divergence of .05 rad. The larger experimental divergence cannot be explained by magnetic fields and must therefore be due to electric fields.

Two mechanisms have been identified for distortion of equipotentials. The first is associated with plasma hydrodynamics when the anode plasma is formed at discrete spots and expands in a two dimensional manner generating bulges on the anode. Since the conductive anode plasma prevents electric field penetration it distorts the equipotential structure close to its surface. Such sooty structure is clearly seen in the shadowbox pinhole images and was also observed using interferometry on the PITHON experiment.[8] The second mechanism is electron beam filamentation in vacuum. The resultant space charge structure introduces azimuthal and radial components to the electric field in addition to the axial field.

The two mechanisms mentioned would have caused large divergences ($\delta\theta \sim .2$ rad) if the electric field would have been compressed against the anode plasma where the ions are launched. The PRD, however, operates by screening the ion beam space charge with the relativistic electrons that pinch and reflex through the anode plasma. This action allows the equipotentials to be spread across the entire diode gap unlike the magnetically insulated diode that only operates at high ion current density when the equipotentials are pushed against the anode plasma. The observed lower $\delta\theta$ of .05 rad is a clear experimental demonstration that even at this average ion source current density of 20 kA/cm^2 the PRD is operating as a space charge enhanced source rather than an electric field enhanced source.

The beam brightness ($JV/\delta\theta^2$) observed for V = 1.2 MV, J = 20 kA/cm^2 and $\delta\theta \sim .05$ rad is $\sim$ 10 TW /cm^{2}rad^2. Scaling this figure up with voltage to the 3 MV level and assuming a factor-of-4 bunching during transport without brightness loss, leads to a modular-beam brightness of about 250 TW/cm^{2}rad^2. If 40% of the solid angle surrounding a pellet is subtended by final-focus exit apertures, on target power densities approaching 100 TW/cm^2 might then be achievable with existing PRDs.

III. EQUITORIAL-PINCH-REFLEX DIODE

A new version of the NRL PRD has been designed to operate on the

radial triplate geometry of PBFA-I. A conceptual schematic is shown in Fig. 3. This diode produces two cylindrically-symmetric sheet beams of electrons which flow from top and bottom by self-magnetic pinching and reflexing action on the anode foil to a common line pinch around the equator of the diode, hence the name equitorial-pinch-reflex diode (EPRD).

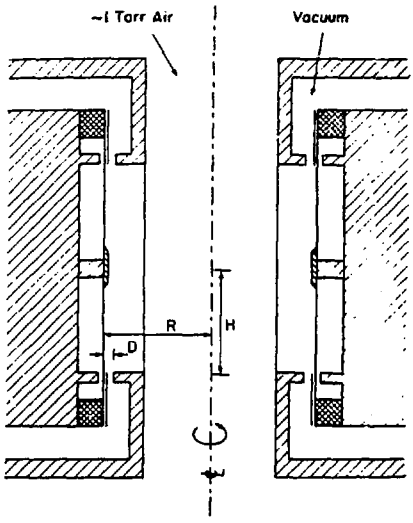

Fig. 3. Equitorial-pinch-reflex diode.

Although this diode appears to be a simple topological variation of the conventional PRD, there are a number of basic conceptual differences. There is no electron-space-charge-density enhancement as occurs with the conventional axial PRD because there is no radially converging electron flow towards the diode axis. This lack of electron convergence leads to a constant ion current density rather than one that increases inversely with the distance from the diode axis as in the axial PRD. These ions produce an azimuthal focusing magnetic field in the gap between the anode and cathode foils which increases proportionally to the distance from the equator. This in turn leads to a natural self-focusing of the ion beam even from a flat anode foil. Any additional spherical curvature of the anode foil simply adds to this natural self-focusing in a manner similar to simple geometric optics. This self-focusing is in contrast to the conventional PRD where the self-magnetic field from the ion current leads to a constant bending angle which must be compensated for by an aspheric focusing anode foil.

The other major difference and advantage of the EPRD over the conventional PRD is that the ratio of ion current to electron current, I_i/I_e, is decoupled from the diode impedance Z. In contrast, in a conventional PRD I_i/I_e scales like R/D and Z scales like D/R, which lead to high ion efficiency only for low impedance diodes (i.e., R/D>>1). For a given anode-cathode gap spacing, D, and diode radius, R, the impedance of the EPRD is proportional to D/R as with the conventional PRD, however, I_i/I_e is proportional to H/D (i.e., the electron path length/the ion path length) and is independent of diode radius or diode impedance. Thus, for any current equal to or above the critical current, the ion production efficiency can be made arbitrarily large by increasing the separation between the two disc cathodes. These properties were verified using a particle-in-cell code.

The EPRD has been tested on NRL's Gamble II generator by driving only the upper half of the diode shown in Fig. 3 in a coaxial-feed geometry. The Gamble diode is designed for negative-polarity operation of Gamble II to allow optical alignment. This arrangement requires diagnostic connections through transit-time-insulator cables installed in the coaxial water line. The anode radius is 7 cm and several anode foil materials including Mylar, polyvinyl acetate and polyethylene are being studied as ion sources. Anode lengths of 5, 10 and 15 cm have been used to provide configurations where the electron path length in the diode is respectively less than, comparable to, and greater than the diode radius. Typical anode-cathode gaps are 3.5 to 6 mm. Diagnostics include x-ray pinhole cameras, probes for measurement of net ion current, total diode current and diode voltage, arrays of ion collector probes, ion beam pinhole imaging to determine beam uniformity, direction and divergence, and various witness plate configurations. A differentially-pumped cylindrical neutralizing gas cell can be deployed inside the cathode-foil cylinder for studying radial convergence of the ion beam under near field-free conditions.

Initial experiments have shown the diode to be an efficient ion source and a good electrical match to the accelerator. Net ion currents on the order of 400 kA have been measured with diode impedances of 1.5-2 Ω. Azimuthally-symmetric electron and ion current flow has been observed. The diode impedance has been shown to be a linear function of anode-cathode gap but practically independent of diode axial height as predicted by theory. Definite limits to the anode surface area which can be uniformly turned on

at a given diode power level have been observed. Filamentation of mode number ~ 100 has been observed at the cathode with concomitant filamentation with mode number ~ 10 in the electron flow down the anode. Enhanced ion production has been observed from anode areas containing these filaments. Imaging of ion beamlets shows time-averaged half-angle divergence of 1-2° from areas not containing filaments while ions from filamented areas have 10-15° time-averaged half-angle divergences, principally in the azimuthal direction. Experiments to reduce the beam filamentation are in progress. Sandia National Laboratory is presently testing a high power diode of similar design on PBFA-I.[6]

IV. ENERGY LOSS EXPERIMENT

Theoretical research[15] indicates that at the ionization levels of ICF pellet plasmas the stopping power of light ions may be enhanced by a factor-of-two over that in the cold target. In this section, measurements of the energy loss of MeV deuterons in plasmas formed by focusing intense Gamble II ion beams (1 MeV, .2 MA, 20 ns) onto subrange-thick targets are presented. The results demonstrate that the stopping power of the heated target is enhanced over that of the cold target.

For these energy-loss measurements, a spherically-contoured PRD (Fig. 4) is used to produce an intense deuteron beam focus about 4 cm

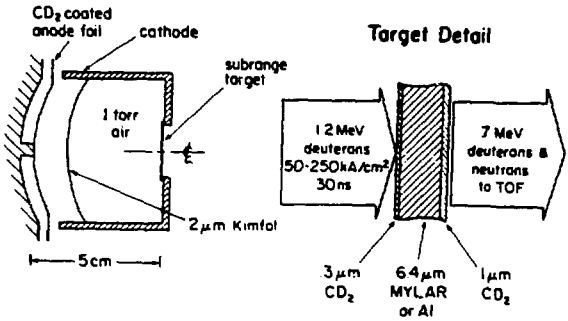

Fig. 4. Experimental set up for energy-loss measurements.

from the anode. The .01 cm thick plastic anode foil is coated with deuterated polyethylene (CD_2) to provide deuterons. A planar anode foil version of the diode is used for lower current density experiments. With planar anodes, the ion beam is focused onto targets about 10 cm from the center of the anode.

The experimental technique for determining the deuteron-energy loss uses neutron time-of-flight (TOF) with a multilayered target.[9] The target consists of a subrange stopping foil sandwiched between .3-μm and 1.0-μm thick layers of CD_2 (Fig. 4). Measurements of the d-d neutron TOF from the two CD_2 targets are used to determine both the incident deuteron energy and the deuteron energy loss in the stopping foil on each shot. Neutrons are detected in the forward-beam direction and reaction kinematics[16] are used to extract deuteron energies. The thickness of the stopping foil is adjusted so that neutrons from the two CD_2 targets can be resolved. In these experiments, 6.4-μm Mylar and aluminum stopping foils are used.

Figure 5 shows a typical trace from the neutron TOF detector.

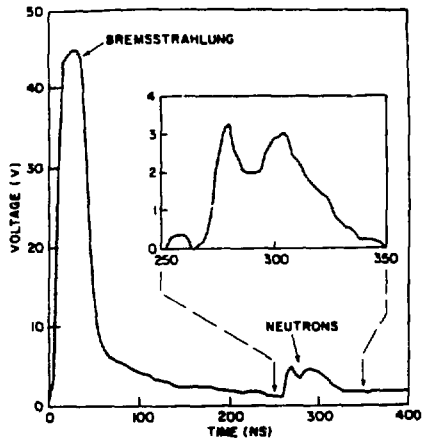

Fig. 5. Neutron TOF trace for Mylar stopping foil, spherical diode and 7.6 m flight path.

Bremsstrahlung radiation from the diode saturates the detector output, but neutron responses from the CD_2 targets are TOF delayed and are resolved about 260 ns after the bremsstrahlung signal. Neutrons are emitted primarily during the time of high voltage and current so that the neutron output is maximum at peak ion power. The time interval between the peak of the ion power and the peak of the first neutron pulse therefore determines the neutron energy from the front CD_2 target and, by kinematic calculation, the incident deuteron energy. A small correction (< 5%) is made to the TOF measurement for the flight time of deuterons from the anode to the target. The neutron signal is shown in the insert of Fig. 5. The flat background from the bremsstrahlung tail has been subtracted from the trace in the insert. The time separation of the two neutron peaks provides a direct measure of the deuteron energy loss in the stopping foil.

Focused ion current densities of 50 kA/cm^2 for the planar diode and 250 kA/cm^2 for the spherical diode are estimated for these experiments using previous proton results [14] using the measured total ion currents. Uncertainties of ±30% are assigned to the current densities obtained in this way. The results of stopping-power measurements using both planar and spherical diodes are presented in Fig. 6. For each case, the measurements

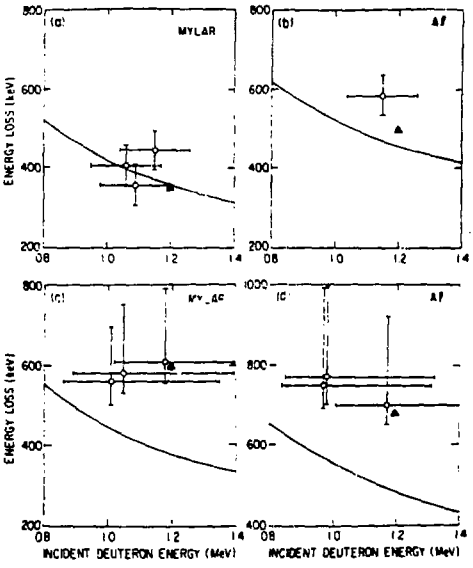

Fig 6. Comparison of energy loss measurements with planar (a and b) and spherical (c and d) diodes with energy losses (curves) calculated for cold-target.

are compared to the cold-target energy loss deduced from measurements of stopping cross sections by Andersen and Ziegler.[17] The measured energy losses are significantly larger than cold-target values in all cases except for the planar diode with a Mylar target. In this case, the measurements are consistent with cold-target values.

The deuteron energy losses deviate from that in a cold-target when sufficient ionization occurs in the stopping medium. The average ionization for aluminum and polyethylene with internal energy density parameterized from "SESAME"[18] are shown in Fig. 7. It is assumed that the free-electron production for Mylar is similar to that for CH_2. The internal energies corresponding to the experimental conditions for planar and spherical diodes are also indicated. It was calculated that ~ 75% of the deposited energy is converted into internal energy during the beam pulse. The rest is in kinetic expansion and radiation losses. This fraction is based on LASNEX hydrocode calculations which model this experiment.[10]

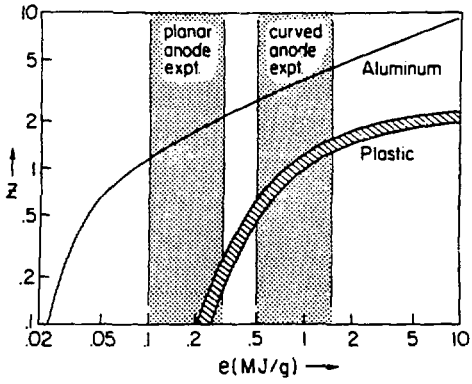

Fig. 7. Average ionization state (z) versus internal energy density (e) for aluminum and plastic (CH_2).

These calculations indicate that the target has expanded to about 2-mm thickness at the peak of the power pulse, and that the electron temperature is 4 to 5 ev at 50 kA/cm^2 and 13 to 17 eV at 250 kA/cm^2 for an aluminum stopping foil. Similar results for Mylar are ~3 eV at 50 kA/cm^2 and 9 to 11 eV at 250 kA/cm^2. The calculated energy losses at peak power are shown as solid triangles in Fig. 6, and are in reasonable agreement with the measurements. For the experimental conditions where a significant number of free electrons are produced in the stopping foil, the measured deuteron stopping is enhanced (Fig. 6b, c and d). If the energy deposition produces less ionization, the measured energy loss is consistent with cold-target stopping (Fig. 6a).

V. TRANSPORT AND FINAL FOCUSING

Intense light-ion beam transport in z-discharge channels provides accelerator standoff from ICF targets and allows time-of-flight bunching of the beam to higher intensity. Stability constraints combined with channel expansion and beam-energy loss constraints define an operational window for ion transport. The stability constraints are derived from the requirements to avoid significant growth of the electron-beam ion two-stream instability, the beam-filamentation instability and the channel-filamentation instability.[19] The channel-expansion constraint results from demanding that the $\underset{\sim}{J}\times\underset{\sim}{B}$-driven radial expansion of the channel occurs on a time scale longer than the beam-pulse duration.[20] Finally, the beam energy-loss constraint requires that no more than 25% of the beam energy is lost during transport.

The constraints have been derived for arbitrary beam-ion species in

order to evaluate the advantages of higher-atomic-weight ions. The beam energy, beam radius and channel density are also free parameters which have been varied in order to determine their effects on the operational window. In all cases, the channel gas was taken as deuterium. This allows the use of a simple model for channel heating and has the advantage of reduced radial acceleration due to the passing beam at the same stopping-power as hydrogen.

Results for beams of H^+, D^+, He^{+2} and C^{+6} show that a larger operational window exists for the higher-atomic-weight species. This is a consequence of their lower currents at equivalent transported power levels. Raising the channel density somewhat above the optimum for minimum beam-energy loss during transport relaxes the two-stream and channel-filamentation stability constraints and the channel-expansion constraint while only slightly modifying the energy-loss constraint. Increasing the beam radius relaxes the two-stream stability constraint and considerably reduces the channel-expansion and beam energy-loss constraints.

It is determined that multi-terawatt beams can be transported a few meters in large-radius channels with beam divergence half angles of .1 to .2 radians. Such angles are presently attainable with PRDs. If time-of-flight bunching during transport and final focusing after transport are employed, less than 10 (and as few as 4) channels are required to deliver the power needed to ignite a pellet. Such a system is conceptually illustrated in Fig. 1.

Theoretical results show factor-of-ten increases in final-focused ion-current density for beams transported in hollow channels. Channels which carry discharge current in the channel interior result in beam-brightness loss during transport and hence cannot be compressed as well by the final focusing cell. Focusing cells which are 1/8 of an ion-betatron-wavelength long focus the beam an additional 1/8-wavelength beyond the exit of the focusing cell. This 1-2 cm drift length is the stand-off distance separating the cell exit from the pellet. High plasma densities can be employed in the short focusing cell without excessive beam-energy loss in order that the plasma-MHD response can be minimized. These high densities combined with a thin transmission foil at the exit of the cell discourage pellet preheat from focusing-cell plasma plumes.

A final-focus system was designed and fielded on the Gamble II

accelerator.[12] Figure 8 shows a schematic representation of the channel.

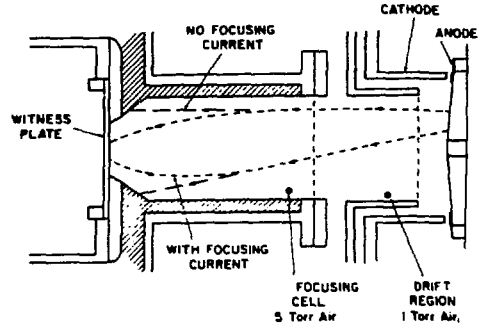

Fig. 8. Final focusing experiment mounted on front of Gamble II diode.

A discharge of ~ 100 kA was initiated by an external capacitor bank along the Lexan insulator (shaded region in Fig. 8) which was filled with 5-10 Torr of air. Channel currents were chosen to match a 1/4 betatron wavelength for the ions with the 8 cm channel length. No attempt in these early proof-of-principle experiments was made to synchronize the ion beam injection with the time dependent channel current density distribution. A convex pinch-reflex type anode was used to partially offset the self pinching of the ion beam in the diode and provide a nearly parallel trajectory injected ion beam. When aluminum witness plates were used, rear surface spall only appeared over the aperture region when the focusing current was turned on. Further experiments with shadowboxes placed downstream of the aperture confirmed that no large scale mixing of the ion orbits in the 1/4 betatron wavelength focusing cell occurred during focusing. Further experiments where the channel current distribution is optimized for a given beam injection condition are planned. Eventually, experiments will be performed with this final-focus system placed at the exit of the transport system.

REFERENCES

+Work supported by Department of Energy, Washington, DC 20545 and Defense Nuclear Agency, Washington, DC 20305
*JAYCOR, Inc., 205 S. Whiting St., Alexandria, VA 22304
**Science Application, Inc., 8400 Westpark Drive, McLean, VA 22101

[1] G. W. Kuswa, J. P. Quintenz, D. B. Seidel, D.J. Johnson, C. W. Mendel, Jr., E. J. T. Burns, D. Fehl, R. J. Leeper, F. C. Perry, P. A. Miller, M. M. Widner, and A. V. Farnsworth, Jr., in the Proceeding of the 4th Int. Conf. on High-Power Electron and Ion-Beam Research and Technology, Palaiseau, France (1981), p.3.

[2] D. Mosher, D. G. Colombant, S. A. Goldstein and P. F. Ottinger, ibid., p. 19.

[3] F. L. Sandel, S. J. Stephanakis, F. C. Young and W. F. Oliphant, ibid., p. 129.

[4] P. F. Ottinger, S. A. Goldstein and D. Mosher, 1980 IEEE Int. Conf. on Plasma Science, Madison, Wisconsin (1980), p. 95; S. A. Goldstein, D. G. Colombant, D. Mosher, P. F. Ottinger and F. Sandel, in the Proceeding of the 4th Int. Conf. on High-Power Electron and Ion-Beam Research and Technology, Palaiseau, France (1981), p. 113.

[5] F. L. Sandel, private communication; R. J. Barker and S. A. Goldstein, Bull. Am. Phys. Soc. 26, 921 (1981).

[6] J. N. Olsen, private communication.

[7] S. J. Stephanakis, S. A. Goldstein, P. F. Ottinger, D. Mosher, Bull. Am. Phys. Soc. 26, 921 (1981).

[8] F. C. Young, G. Cooperstein, S. A. Goldstein, D. Mosher, S. J. Stephanakis, W. F. Oliphant, and J. R. Boller, J. Maenchen, R. D. Genuario and R. N. Stringfield, NRL Memorandum Report 4726 (1981).

[9] F. C. Young, D. Mosher, S. J. Stephanakis, S. A. Goldstein, and T. A. Mehlhorn, 1982 IEEE Int. Conf. on Plasma Science, Ottawa, Canada.

[10] T. A. Mehlhorn, private communication.

[11] P. F. Ottinger, D. Mosher and S. A. Goldstein, 1982 IEEE Int. Conf. on Plasma Science, Ottawa, Canada.

[12] R. A. Meger, Shyke A. Goldstein, P. F. Ottinger, D. Mosher, S. J. Stephanakis, and F. C. Young, Bull. Am. Phys. Soc. 26, 921 (1981).

[13] S. A. Goldstein, G. Cooperstein, R. Lee, D. Mosher and S. J. Stephanakis, Phys. Rev. Lett. 40, 1504 (1978).

[14] G. Cooperstein, S. A. Goldstein, D. Mosher, R. J. Barker, J. R. Boller, D. G. Colombant, A. Drobot, R. A. Meger, W. F. Oliphant, P. F. Ottinger, F. L. Sandel, S. J. Stephanakis and F. C. Young, in Laser Interaction and Related Phenomena, edited by H. Schwarz, H. Hora, M. Lubin and B. Yaakobi (Plenum, New York, 1981), Vol. 5 p. 105.

[15] T. A. Mehlhorn, J. Appl. Phys. 52, 6522 (1981); E. Nardi, E. Peleg and Z. Zinamon, Appl. Phys. Lett., 39, 46 (1981); D. Mosher in ERDA Summer Study of Heavy Ions for Inertial Fusion LBL-5543, 1976, p. 39 (unpublished).

[16] H. Liskien and A. Paulsen, Atomic and Nuclear Data Tables 15, 57 (1975).

[17] H. H. Andersen and J. F. Ziegler, The stopping and Ranges of Ions in Matter, Vol. 3 (Pergamon Press, NY 1977).

[18] B. I. Bennett, J. D. Johnson, G. I. Kerly, G. T. Rood, "Recent Developments in the SESAME Equation-of-State Library,." Los Alamos Scientific Laboratory Report LA 7130, 1978 (unpublished).

[19] P. F. Ottinger, S. A. Goldstein and D. Mosher, NRL Memo Report 4548, July 1981.

[20] D. Mosher, D. G. Colombant and S. A. Goldstein, Comments Plasma Physics, 6, 101 (1981).